

# Moving-Resting Process with Measurement Error in Animal Movement Modeling

Chaoran Hu, Vladimir Pozdnyakov, and Jun Yan  
Department of Statistics, University of Connecticut

## **Abstract**

Statistical modeling of animal movement is of critical importance. The continuous trajectory of an animal's movements is only observed at discrete, often irregularly spaced time points. Most existing models cannot handle the unequal sampling interval naturally and/or do not allow inactivity period such as resting or sleeping. The recently proposed moving-resting (MR) model is a Brownian motion governed by a telegraph process, which allows periods of inactivity in one state of the telegraph process. It is promising in modeling the movements of predators with long inactive periods such as mountain lions, but the lack of accommodation of measurement errors seriously prohibits its applications in practice. Here we incorporate measurement errors in the MR model and derive basic properties of the model. Inferences are based on a composite likelihood using the Markov property of the chain formed by every other observations. The performance of the method is validated in finite sample simulation studies. Application to the movement data of a mountain lion in Wyoming illustrates the utility of the method.

**KEYWORDS:** Composite likelihood; Dynamic programming; Markov process

# 1 Introduction

Statistical modeling of animal movement is of great importance in addressing fundamental questions about space use, movement, resource selection, and behavior in animal ecology (Hooten et al., 2017). The explosion of telemetric data on animal movement from the recent advancements in tracking and observation technologies presents a storm of opportunities and challenges (Cagnacci et al., 2010; Patterson et al., 2017). Due to battery life limitation, the continuous trajectory of an animal’s movement is typically only observed at discrete, often irregularly spaced time points. As a result, discrete-time models such as the state space model (e.g., Jonsen et al., 2005; Patterson et al., 2008; McClintock et al., 2012) are not realistic. Continuous-time models based on stochastic differential equation (SDE) (e.g., Preisler et al., 2004; Horne et al., 2007; Brillinger, 2010) can handle the irregular spacing naturally. Nonetheless, most existing works assume perpetual motion and cannot accommodate periods of inactivity. On the time scale of most telemetry data, most animals alternate between periods of continuing movement (foraging) and periods of rest (e.g., eating or sleeping) (Mashanova et al., 2010; Ueno et al., 2012). Realistic continuous-time models that accommodate inactive periods are needed.

A promising model to accommodate inactive periods is the recently proposed moving-resting (MR) process (Yan et al., 2014). The MR process is a Brownian motion governed by a telegraph or on-off process (e.g., Zacks, 2004). Specifically, it allows an animal to alternate between a moving state, during which it moves in a Brownian motion (BM), and a resting state, during which it remains motionless. The switch between the two states is characterized governed by a telegraph process, where the holding time (or duration) of each state is assumed to follow an exponential distribution. The memoryless holding time makes the underlying state process a continuous time Markov Chain. As a consequence, the MR process can be analyzed with the help of hidden Markov model (HMM) tools (Cappé et al., 2005). The MR process is a first step towards more realistic animal movement modeling with discretely observed telemetry data where the trajectories contain evident motionless

segments. Implementation of likelihood based inferences for the MR process based on dynamic programming (Pozdnyakov et al., 2019) is publicly available in an R package `smam` (Yan et al., 2019).

A major limitation in applying the MR model to animal movement data is that it does not accommodate the measurement error of telemetric devices. Adding measurement error to a Brownian motion model is not crucial as long as the measurement error is small in comparison to the total standard deviation of the increments of the Brownian motion between two consecutive time points (Pozdnyakov et al., 2014). In such cases, discarding the measurement error would not produce significant bias. The impact of the measurement errors on inferences about MR processes, however, is much greater. For a given sequence of hidden states, the likelihood is a product of both densities *and* probabilities. If two observed locations are exactly the same, that is, the trajectory is flat over time, then the animal is known to be motionless between the two time points. The likelihood contribution is the probability of staying in the motionless state instead of the density of the increment at zero. Adding even a tiny bit of noise would remove those flat pieces of the trajectory and, hence, cause drastic bias in the likelihood estimator of the parameters. One possible approach is to round the observed locations, which introduces flat pieces. The number of such pieces, however, depends greatly on the rounding level, which there are no obvious rules to choose. A detailed illustration of the issue is in the next Section.

Dealing with added noise in the MR process is challenging because it invalidates the Markov property of the joint location-state process. The transition density from one time to the next time point can in principle be obtained from convoluting the results of the MR process (Yan et al., 2014) with normally distributed measurement errors, although computationally very intensive. Lack of Markov property of the joint location-state process means the true likelihood cannot be easily formed by multiplying these transition densities. Because the measurement errors are continuous, the dynamic programming tools of HMM based on a finite number of hidden states (Cappé et al., 2005) are not applicable. The generic

simulation based inferences such as iterated filtering (Ionides et al., 2011, 2015) or particle Markov chain Monte Carlo (Andrieu et al., 2010), available in R package `pomp` (King et al., 2016) are not feasible from our investigation due to the complexity of the MR process with measurement error.

Our contribution is a toolbox for applying the MR process with measurement error to animal movement modeling. First, we show that discarding the measurement error, even tiny bit ones, cause severe bias in estimation, and that rounding does not provide any satisfactory solution. To make inferences for MR process with measurement error, we establish that, after thinning every other observation, the remaining observations are location-state Markov. This facilitates a composite likelihood which contains two true likelihood components, one based on odd-numbered observations and the other based on even-numbered observations. The true likelihood of each component is computed with dynamic programming. The variance of the maximum composite likelihood estimator can be estimated by a sandwich variance estimator or through parametric bootstrap. The validity of the approach is confirmed in a simulation study. We then apply the approach to model the movement data of mountain lion in Wyoming, whose trajectory is known to have long inactive periods. Discussed methods were implemented as R package `smam` (Yan et al., 2019) with efficient C++ code.

## 2 Moving-Resting Process

The MR process is a Brownian motion with an infinitesimal variance that is governed by an alternating renewal process with two different holding times. Let random variables  $\{M_i\}_{i \geq 1}$  be independent exponential variables with rate  $\lambda_1$ , and  $\{R_i\}_{i \geq 1}$  be independent exponential variables with rate  $\lambda_0$ . These are the holding times. There are two possible alternating sequences of the holding times,  $(M_1, R_1, M_2, R_2, \dots)$  or  $(R_1, M_1, R_2, M_2, \dots)$ . Which one represents a particular realization depends on an initial distribution. A continuous time state process,  $S(t)$ ,  $t \geq 0$ , takes only two values, 0 and 1, and it is defined by the holding

times. In particular, for sequence  $(M_1, R_1, M_2, R_2, \dots)$ , if there exists  $k \geq 0$  such that

$$\sum_{j=1}^k (M_j + R_j) < t \text{ but } \sum_{j=1}^k (M_j + R_j) + M_k \geq t,$$

then  $S(t) = 1$ ; otherwise,  $S(t) = 0$ . For sequence  $(R_1, M_1, R_2, M_2, \dots)$ , if there exists  $k \geq 0$  such that

$$\sum_{j=1}^k (R_j + M_j) < t \text{ but } \sum_{j=1}^k (R_j + M_j) + R_k \geq t,$$

then  $S(t) = 0$ , otherwise,  $S(t) = 1$ . It is well-know that the state process is stationary, if the initial probability of  $\{S(0) = 1\}$  is set as

$$p_1 = \frac{\lambda_0}{\lambda_0 + \lambda_1},$$

and the initial probability of  $\{S(0) = 0\}$  is set as  $p_0 = 1 - p_1$ .

An MR process  $X(t)$ ,  $t \geq 0$ , is defined by a stochastic differential equation

$$dX(t) = \begin{cases} \sigma dB(t) & \text{if } S(t) = 1, \\ 0 & \text{if } S(t) = 0, \end{cases}$$

where  $B(t)$  is the standard Brownian motion, and  $\sigma$  is a volatility parameter. It is important to note that  $\{X(t)\}_{t \geq 0}$  itself is not Markov, but the location-state process  $\{X(t), S(t)\}$  is with stationary increments.

Properties and inferences of the MR process has been studied in [Yan et al. \(2014\)](#) and [Pozdnyakov et al. \(2019\)](#). A key elements is the distribution of occupation times, that is, the total time spent in the moving state by time  $t$

$$M(t) = \int_0^t S(s) ds,$$

and the total time spent in the resting state  $R(t) = t - M(t)$ . Let  $P_i(\cdot)$  be the conditional

probability  $P(\cdot|S(0) = i)$ . [Zacks \(2004\)](#) derived computationally efficient formulas for the following (defective) densities

$$p_{11}(w, t)dw = P_1(M(t) \in dw, S(t) = 1),$$

$$p_{10}(w, t)dw = P_1(M(t) \in dw, S(t) = 0),$$

$$p_{01}(w, t)dw = P_0(R(t) \in dw, S(t) = 1),$$

$$p_{00}(w, t)dw = P_0(R(t) \in dw, S(t) = 0),$$

where  $0 < w < t$ .

Having this at hand, one can derive the marginal distribution of the increment  $X(t) - X(0)$ . Without loss of generality, let  $X(0)$  to be 0, and  $X(t)$  becomes the increment from time 0 to time  $t$ . Then, the joint distribution of the increment  $X(t)$  and  $S(t)$ ,  $t > 0$ , is given by

$$P_1(X(t) \in dx, S(t) = 1) = h_{11}(x, t)dx,$$

$$P_1(X(t) \in dx, S(t) = 0) = h_{10}(x, t)dx,$$

$$P_0(X(t) \in dx, S(t) = 0) = h_{00}(x, t)dx + e^{-\lambda_0 t} \delta_0(x),$$

$$P_0(X(t) \in dx, S(t) = 1) = h_{01}(x, t)dx,$$

where  $\delta_0(x)$  is the delta function with an atom at 0,  $x \in \mathbb{R}$ , and  $h_{ij}(x, t)$ ,  $i, j \in \{0, 1\}$ , are functions derived in [Yan et al. \(2014\)](#):

$$h_{11}(x, t) = e^{-\lambda_1 t} \phi(x; \sigma^2 t) + \int_0^t \phi(x; \sigma^2 w) p_{11}(w, t) dw,$$

$$h_{10}(x, t) = \int_0^t \phi(x; \sigma^2 w) p_{10}(w, t) dw,$$

$$h_{00}(x, t) = \int_0^t \phi(x; \sigma^2(t - w)) p_{00}(w, t) dw,$$

$$h_{01}(x, t) = \int_0^t \phi(x; \sigma^2(t - w)) p_{01}(w, t) dw.$$

with  $\phi(\cdot; \sigma^2)$  being the density function of normal distribution  $N(0, \sigma^2)$ . The marginal distribution of increment  $X(t)$  can be obtained by summing our  $S(t)$  and  $S(0)$ , which forms the basis of the composite likelihood in [Yan et al. \(2014\)](#). The full maximum likelihood estimation algorithm based on dynamic programming was developed in [Pozdnyakov et al. \(2019\)](#).

For animal movement data In practice, we may never observe the exact values of  $X(t)$ , but  $X(t)$  with added measurement errors. For an MR process, the probability of observing a zero increment is strictly positive. With added noise, even a tiny bit, this feature is destroyed — the probability becomes zero. Rounding can help, but it is not trivial to come up with an appropriate rounding level. [Figure 1](#) (up left) shows the easting/northing coordinates in Universal Transverse Mercator (UTM) of a female lion in 2012 in the Gros Ventre mountain range, Wyoming. The patterns of resting — places where both lines are more or less flat — and moving are readily apparent, which can hardly be captured by any existing model that assumes perpetual movements. The other three panels of [Figure 1](#) show the coordinates of a simulated MR path without noise and with noise of two levels. The pattern is very similar to that in the left panel for the female mountain lion. The similarity is obvious, suggesting that an MR process may be a good model, but as shown next, ignoring the noise is disastrous in estimating the model parameters.

We demonstrate the impact of noise on estimation by a simulation study. Consider an MR process with parameters  $\lambda_1 = 1/hr.$ ,  $\lambda_0 = 0.5/hr.$ ,  $\sigma = 1km/hr.^{1/2}$ . The measurement errors were independent Gaussian noise with standard deviation  $0.05km$  (1/20 of volatility) and  $0.01km$  (1/100 of volatility). The time intervals between consecutive observations was 5 hours. We generated 100 dataset, each with 200 observations. The maximum likelihood estimates based on the MR process were obtained for dataset with and without noise, where for data with noise, three levels of rounding were considered, 10, 50, and 100 meters. [Table 1](#) summarizes the parameter estimates based on the 100 replicates. The point estimates are acceptable for the data without noises. For data with noises, however, severe biases are seen



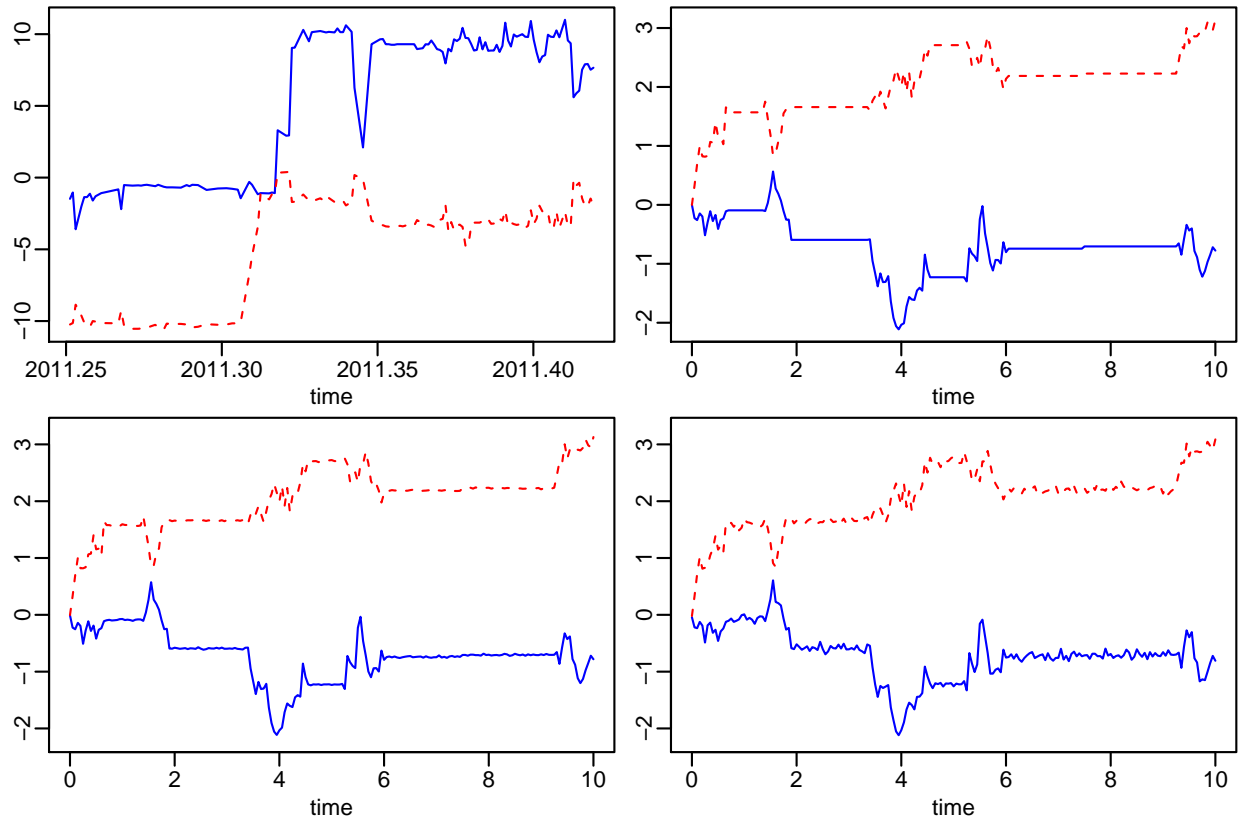


Figure 1: *Up left*: Actual coordinates of a female mountain lion in a two-month period in 2012 in the Gros Ventre mountain range, Wyoming, with most observations separated by 8 hours. The x-axis is time in years. The y-axis is departure from the starting point. The solid blue line is UTM easting ( $km$ ) and the dashed red line is UTM northing ( $km$ ). *Up right*: Coordinates of a realization from a two-dimensional MR process. The two coordinates are dependent because the straight line segments representing resting periods are shared. *Bottom left*: Coordinates of the same realization as up right panel after adding Gaussian noise with standard deviation 0.01. *Bottom right*: Coordinates of the same realization as up right panel after adding Gaussian noise with standard deviation 0.05.

for all three parameters. As the rounding becomes coarser, the biases decrease but remain notable. This is true even for the case with noise standard deviation 0.01km. It is indeed unclear how to choose an appropriate rounding level. An elegant estimation should handle the measurement errors directly.

Table 1: Influence of measurement error on moving-resting process parameter estimation. The true parameter of moving-resting process is  $\lambda_1 = 1/hr$ ,  $\lambda_0 = 0.5/hr$ ,  $\sigma = 1km/hr^{1/2}$ . The measurement error is set as Gaussian noise with standard deviation 0.05 and 0.01. The length of the time intervals between consecutive observations is 5. The number of observations is 200. The number of replication is 100. The mean and empirical standard deviation of estimators under different setups are recorded.

Gaussian noise s.d. ( <i>km</i> )	Rounding ( <i>km</i> )	$\hat{\lambda}_1$		$\hat{\lambda}_0$		$\hat{\sigma}$	
		mean	s.d.	mean	s.d.	mean	s.d.
—	—	1.58	2.29	0.50	0.08	1.08	0.38
0.05	—	21.16	12.21	0.89	0.08	2.73	0.75
	0.01	21.58	9.92	0.89	0.08	2.78	0.68
	0.05	15.08	10.00	0.85	0.08	2.34	0.76
	0.10	9.72	7.70	0.75	0.10	1.98	0.74
0.01	—	22.00	10.82	0.83	0.07	2.89	0.75
	0.01	17.61	9.29	0.80	0.07	2.62	0.74
	0.05	4.95	4.60	0.61	0.09	1.57	0.65
	0.10	2.24	3.15	0.54	0.09	1.18	0.47

### 3 Moving-Resting Process with Measurement Error

Suppose the observations are recorded at times  $t_0 = 0, t_1, \dots, t_n$ . Let  $\{\epsilon_k\}_{k=0, \dots, n}$  be independent and identically normally distributed random variables with mean 0 and variance  $\sigma_\epsilon^2$ . An MR process with measurement error (MRME)  $Z(t)$  at each time point is the superimposition of a measurement error and the exact location. That is, the observed location at  $t_k$ ,  $Z(t_k)$ , is

$$Z(t_k) = X(t_k) + \epsilon_k, \quad (1)$$

where  $\epsilon_k$ 's are independent  $N(0, \sigma_\epsilon^2)$  noises.

Some properties of the process  $\{Z(t_k)\}_{k=0, \dots, n}$  are in order. Obviously, it is not Markov. Neither is the location-state process  $\{Z(t_k), S(t_k)\}_{k=0, \dots, n}$ . Nonetheless, the discretely observed process  $\{Z(t_{2k}) - Z(t_{2k-1}), S(t_{2k})\}_{k=1, \dots, [n/2]}$  is Markov. This is an important property which is used to construct a composite likelihood in the next section. We show this property by demonstrating that the distribution of  $(Z(t_{2k+2}) - Z(t_{2k+1}), S(t_{2k+2}))$  depends only on

state  $S(t_{2k})$ .

First, let us calculate the marginal distribution of  $Z(t) - Z(0)$  (the increment of  $\{Z(t)\}_{t \geq 0}$  from time 0 to time  $t$ ). Consider  $\Delta Z(t) = Z(t) - Z(0) = X(t) - X(0) + \xi$ , where  $\xi \sim N(0, 2\sigma_\epsilon^2)$  independent of process  $(X(t), S(t))$ . Note that,  $Z(t_{2k+2}) - Z(t_{2k+1}) = X(t_{2k+2}) - X(t_{2k+1}) + \epsilon_{2k+2} - \epsilon_{2k+1}$ , and  $\{\epsilon_{2k+2} - \epsilon_{2k+1}\} \sim N(0, 2\sigma_\epsilon^2)$ . Without loss of generality, we assume that  $X(0) = 0$ . Denote

$$g_{ij}(z, t) = P_i(\Delta Z(t) \in dz, S(t) = j) / dz,$$

where  $i, j = \{1, 0\}$ . Then, we get that

$$\begin{aligned} g_{11}(z, t) dz &= P_1(\Delta Z(t) \in dz, S(t) = 1) \\ &= \int_{\mathbb{R}} P_1(X(t) + \xi \in dz, S(t) = 1, \xi \in dx) \\ &= \int_{\mathbb{R}} P_1(X(t) \in dz - x, S(t) = 1) \phi(x; 2\sigma_\epsilon^2) dx \\ &= \int_{\mathbb{R}} h_{11}(z - x, t) dz \phi(x; 2\sigma_\epsilon^2) dx, \end{aligned}$$

where, as before,  $\phi(\cdot; \sigma^2)$  is the density function of  $N(0, \sigma^2)$ . Similarly, one can get that

$$\begin{aligned} g_{10}(z, t) &= \int_{\mathbb{R}} h_{10}(z - x, t) \phi(x; 2\sigma_\epsilon^2) dx, \\ g_{01}(z, t) &= \int_{\mathbb{R}} h_{01}(z - x, t) \phi(x; 2\sigma_\epsilon^2) dx, \\ g_{00}(z, t) &= \int_{\mathbb{R}} h_{00}(z - x, t) \phi(x; 2\sigma_\epsilon^2) dx + e^{-\lambda_0 t} \phi(z; 2\sigma_\epsilon^2). \end{aligned}$$

Next, let us denote

$$\tau_{ij}(t) = P_i(S(t) = j).$$

It is easy to see

$$\tau_{01}(t) = P_0(S(t) = 1)$$

$$\begin{aligned}
&= \sum_{n=0}^{\infty} \left[ P \left( \sum_{k=1}^{n+1} R_k + \sum_{k=1}^n M_k \leq t \right) - P \left( \sum_{k=1}^{n+1} R_k + \sum_{k=1}^{n+1} M_k \leq t \right) \right] \\
&= \sum_{n=0}^{\infty} H(t, n, \lambda_1, n+1, \lambda_0).
\end{aligned}$$

Here,  $\{M_i\}_{i \geq 1}$  and  $\{R_i\}_{i \geq 1}$  are defined in Section 2, and a summation over an empty set is 0. The functions  $H(t, n, \lambda_1, n+1, \lambda_0)$  were investigated in Hu et al. (2019), where a computationally efficient algorithm for computing these functions was derived. Using similar technique, we obtain that

$$\begin{aligned}
\tau_{10}(t) &= \sum_{n=0}^{\infty} H(t, n, \lambda_0, n+1, \lambda_1), \\
\tau_{00}(t) &= \sum_{n=0}^{\infty} H(t, n, \lambda_0, n, \lambda_1), \\
\tau_{11}(t) &= \sum_{n=0}^{\infty} H(t, n, \lambda_1, n, \lambda_0).
\end{aligned}$$

Finally, we are ready to present the transition density at  $(Z(t) - Z(u), S(t))$  given  $S(0)$ , where  $0 < u < t$ ,  $Z(u) = X(u) + \xi$ ,  $Z(t) = X(t) + \eta$ , and  $\xi$  and  $\eta$  are independent measurement errors with  $N(0, \sigma_\epsilon^2)$  distribution. Using the Markov property of the location-state process  $(X(t), S(t))$  and independence of the added noise, one can get that

$$f(Z(t) - Z(u), S(t) = j | S(0) = i) = \sum_{k=0}^1 \tau_{ik}(u) g_{kj}(Z(t) - Z(u), t - u),$$

where  $i, j \in \{0, 1\}$ .

In conclusion, let us note that real-world animal movement data sets are two-dimensional. The formulas from above can be generalized to a  $d$ -dimensional case. They are given in Appendix A.

## 4 Composite Likelihood Estimation

Since the full likelihood is unavailable, we resort to composite likelihood to estimate the parameters (Lindsay, 1988). A composite likelihood is a weighted product of likelihood segments

$$\text{CL} = \prod_{k=1}^K L_k^{w_k},$$

where  $L_k$  is the true likelihood of the  $k$ -th data segment with a non-negative weight  $w_k$ ,  $k = 1, \dots, K$ , and  $K$  is the number of segments depending on the construction of the CL. The weights can be useful, for example, in pairwise likelihood when some pairs with stronger dependence contribute more than other pairs. Suppose that the location-state observations are denoted as

$$\mathbf{Z} = (Z(t_0), Z(t_1), \dots, Z(t_n))$$

$$\mathbf{S} = (S(t_0), S(t_1), \dots, S(t_n)).$$

The observed data only contains  $\mathbf{Z}$ . We propose two ways to construct composite likelihood.

### 4.1 Two-piece Composite Likelihood

The likelihood of increment-state observations at even time points

$$\mathbf{Z}_{\text{even}} = (Z_2, \dots, Z_{2[n/2]}),$$

$$\mathbf{S}_{\text{even}} = (S(t_0), S(t_2), \dots, S(t_{2[n/2]})),$$

where  $Z_k = Z(t_k) - Z(t_{k-1})$  is given by

$$L(\mathbf{Z}_{\text{even}}, \mathbf{S}_{\text{even}}; \boldsymbol{\theta}) = \nu(S(t_0)) \prod_{k=1}^{[n/2]} f(Z_{2k}, S(t_{2k}) | S(t_{2k-2})),$$

where  $[\cdot]$  is the integer function,  $\boldsymbol{\theta} = (\lambda_1, \lambda_0, \sigma, \sigma_\epsilon)$  and  $\nu(S(t_0))$  is the initial distribution that is assumed to be stationary. In practice,  $\mathbf{S}_{even}$  are hidden states. So, we need the likelihood of the increment process  $\mathbf{Z}_{even}$ . This can be obtained by taking sum over all possible state trajectories:

$$L(\mathbf{Z}_{even}; \boldsymbol{\theta}) = \sum_{S(t_0), S(t_2), \dots, S(t_{2[n/2]}) \in \{0,1\}} L(\mathbf{Z}_{even}, \mathbf{S}_{even}; \boldsymbol{\theta}).$$

The cardinality of the set of the state trajectories is  $2^{[n/2]+1}$ . But it is still can be efficiently evaluated with help of dynamic programming, specifically, by the forward algorithm.

First, let us define the forward variables by

$$\begin{aligned} \alpha(\mathbf{Z}_{even}(t_{2k}), S(t_{2k}), \boldsymbol{\theta}) &= \sum_{S(t_0), S(t_2), \dots, S(t_{2k-2}) \in \{0,1\}} \nu(S(t_0)) \\ &\quad \times \prod_{j=1}^k f(Z(t_{2j}) - Z(t_{2j-1}), S(t_{2j}) | S(t_{2j-2})), \end{aligned}$$

where  $\mathbf{Z}_{even}(t_{2k}) = (Z(t_0), Z(t_2), \dots, Z(t_{2k}))$  and  $k = 1, \dots, [n/2]$ , and the initial forward variable  $\alpha(\mathbf{Z}_{even}(t_0), S(t_0), \boldsymbol{\theta}) = \nu(S(t_0))$ . Then, it is easy to see that the forward variables satisfy the following recursive relationship:

$$\begin{aligned} \alpha(\mathbf{Z}_{even}(t_{2k+2}), S(t_{2k+2}), \boldsymbol{\theta}) &= \sum_{S(t_{2k}) \in \{0,1\}} \alpha(\mathbf{Z}_{even}(t_{2k}), S(t_{2k}), \boldsymbol{\theta}) \\ &\quad \times f(\mathbf{Z}_{even}(t_{2k+2}) - \mathbf{Z}_{even}(t_{2k+1}), S(t_{2k+2}) | S(t_{2k})). \end{aligned}$$

This allows us to compute the likelihood in linear time with respect to  $n$  time, because

$$L(\mathbf{Z}_{even}; \boldsymbol{\theta}) = \sum_{S(t_{2[n/2]}) \in \{0,1\}} \alpha(\mathbf{Z}_{even}(t_{2[n/2]}), S(t_{2[n/2]}), \boldsymbol{\theta}).$$

Now, when the sample size  $n$  is large, the likelihood tends to be too small to be distinguished

from zero by computer. To address the underflow problem, one should use the normalized forward algorithm. More specifically, let us introduce the normalized forward variables as

$$\bar{\alpha}(\mathbf{Z}_{\text{even}}(t_{2k}), S(t_{2k}), \boldsymbol{\theta}) = \frac{\alpha(\mathbf{Z}_{\text{even}}(t_{2k}), S(t_{2k}), \boldsymbol{\theta})}{L(\mathbf{Z}_{\text{even}}(t_{2k}); \boldsymbol{\theta})},$$

and let

$$d(\mathbf{Z}_{\text{even}}(t_{2k+2}); \boldsymbol{\theta}) = \frac{L(\mathbf{Z}_{\text{even}}(t_{2k+2}); \boldsymbol{\theta})}{L(\mathbf{Z}_{\text{even}}(t_{2k}); \boldsymbol{\theta})}.$$

Then, the update formulas for normalized forward variable  $\bar{\alpha}(\mathbf{Z}_{\text{even}}(t_{2k}), S(t_{2k}), \boldsymbol{\theta})$  and  $d(\mathbf{Z}_{\text{even}}(t_{2k+2}); \boldsymbol{\theta})$  are given by

$$\begin{aligned} \bar{\alpha}(\mathbf{Z}_{\text{even}}(t_{2k+2}), S(t_{2k+2}), \boldsymbol{\theta}) &= \frac{1}{d(\mathbf{Z}_{\text{even}}(t_{2k+2}); \boldsymbol{\theta})} \\ &\times \sum_{S(t_{2k}) \in \{0,1\}} \bar{\alpha}(\mathbf{Z}_{\text{even}}(t_{2k}), S(t_{2k}), \boldsymbol{\theta}) \\ &\times f(\mathbf{Z}_{\text{even}}(t_{2k+2}) - \mathbf{Z}_{\text{even}}(t_{2k+1}), S(t_{2k+2}) | S(t_{2k})), \end{aligned}$$

and

$$\begin{aligned} d(\mathbf{Z}_{\text{even}}(t_{2k+2}); \boldsymbol{\theta}) &= \sum_{S(t_{2k+2}), S(t_{2k}) \in \{0,1\}} \bar{\alpha}(\mathbf{Z}_{\text{even}}(t_{2k}), S(t_{2k}), \boldsymbol{\theta}) \\ &\times f(\mathbf{Z}_{\text{even}}(t_{2k+2}) - \mathbf{Z}_{\text{even}}(t_{2k+1}), S(t_{2k+2}) | S(t_{2k})). \end{aligned}$$

Finally, the likelihood function is given by

$$\log L(\mathbf{Z}_{\text{even}}(t_{2k}); \boldsymbol{\theta}) = \sum_{k=1}^{\lfloor n/2 \rfloor} \log d(\mathbf{Z}_{\text{even}}(t_{2k}); \boldsymbol{\theta}). \quad (2)$$

In a similar fashion, one can compute the likelihood of the observed increments at the odd time points  $\mathbf{Z}_{\text{odd}} = (Z_1, Z_3, \dots, Z_{2\lfloor (n+1)/2 \rfloor - 1})$ . Adding two log-likelihoods together we

get the following composite log-likelihood:

$$cl((Z(t_0), \dots, Z(t_n)); \boldsymbol{\theta}) = \log(L(\mathbf{Z}_{\text{even}}; \boldsymbol{\theta})) + \log(L(\mathbf{Z}_{\text{odd}}; \boldsymbol{\theta})). \quad (3)$$

The maximum composite likelihood estimator (MCLE) of  $\boldsymbol{\theta}$  is the maximizer  $\hat{\boldsymbol{\theta}}$  of (3).

## 4.2 Marginal Composite Likelihood

The second approach is to use the one-step transition density with the dependence between two consecutive increments discarded. If  $\mathbf{S}$  were observed, for  $i, j \in \{0, 1\}$ , the likelihood of each pair of consecutive location-state observations

$$(\{Z(t_{k-1}), S(t_{k-1}) = i\}, \{Z(t_k), S(t_k) = j\})$$

is

$$\nu(S(t_{k-1}) = i)g_{ij}(Z(t_k) - Z(t_{k-1}), t_k - t_{k-1}),$$

where  $\nu(\cdot)$  is the stationary distribution of state process  $\{S(t)\}_{t \geq 0}$ . Since  $\mathbf{S}$  is unobserved, the likelihood of  $(Z(t_{k-1}), Z(t_k))$  is

$$\sum_{j=0}^1 \sum_{i=0}^1 \nu(S(t_{k-1}) = i)g_{ij}(Z(t_k) - Z(t_{k-1}), t_k - t_{k-1}).$$

The marginal composite log-likelihood is

$$cl^*((Z(t_0), \dots, Z(t_n)); \boldsymbol{\theta}) = \sum_{k=1}^n \log \left[ \sum_{j=0}^1 \sum_{i=0}^1 \nu(S(t_{k-1}) = i)g_{ij}(Z(t_k) - Z(t_{k-1}), t_k - t_{k-1}) \right]. \quad (4)$$

Since the dependence among the increments is discarded, the resulting estimator is expected to be less efficient if the dependence is stronger.



### 4.3 Variance Estimation

To make inferences about  $\boldsymbol{\theta}$ , we need the variance of  $\hat{\boldsymbol{\theta}}$ . It can be estimated by parametric bootstrap with the time points fixed easily because simulating from the MRME process is simple. The general approach of parametric bootstrap is given as Algorithm 1.

---

**Algorithm 1:** Estimated standard error from parametric bootstrap

---

**input** : Observed data; number of resampling  $M$ .

· Fit model to get the parameter estimates;

**for**  $m = 1$  to  $M$  **do**

    · Use the estimated parameters to generate a bootstrap sample on the observed time grids;

    · Fit model to the bootstrap sample to get bootstrap estimate;

**end**

· Make inference based on empirical distribution from these bootstrap estimators.

---

Alternatively, we can estimate the variance by inverting the observed Godambe information matrix (Godambe, 1960)

$$G(\boldsymbol{\theta}) = H(\boldsymbol{\theta})J(\boldsymbol{\theta})^{-1}H(\boldsymbol{\theta}),$$

where

$$H(\boldsymbol{\theta}) = \mathbf{E} \left[ -\frac{\partial^2}{\partial \boldsymbol{\theta}^2} cl((Z(t_0), \dots, Z(t_n)); \boldsymbol{\theta}) \right],$$

and

$$J(\boldsymbol{\theta}) = \text{Var} \left[ \frac{\partial}{\partial \boldsymbol{\theta}} cl((Z(t_0), \dots, Z(t_n)); \boldsymbol{\theta}) \right].$$

Practically,  $H(\boldsymbol{\theta})$  is estimated by the Hessian matrix of the negative composite likelihood evaluated at  $\hat{\boldsymbol{\theta}}$ . Calculation of  $J(\boldsymbol{\theta})$  is more difficult as there is no replicated data to estimate this variance. Parametric bootstrap can be applied to evaluate  $J(\boldsymbol{\theta})$  as the empirical variance of gradient of composite likelihood from a large number of bootstrap samples. Finally,  $\text{Var}(\hat{\boldsymbol{\theta}})$  can be obtained by the inverse of  $G(\hat{\boldsymbol{\theta}})$  (e.g., Varin et al., 2011). However, according to our simulation result, this approach does not perform as good as parametric bootstrap approach.

## 5 Simulation Study

We ran several simulations to check performance of the MCLE based on both the marginal composite likelihood and the two-piece composite likelihood. The objective of this study is threefold: (1) to see if the procedures successfully recovers the model parameters, (2) to verify that standard errors can be obtained with help of parametric bootstrap, and (3) to compare performance of the marginal method to the two-piece one.

First, we generated movement data using MRME model described by equation (1). The model parameters were set to be  $\lambda_1 = 1$ ,  $\lambda_0 = 0.5$ ,  $\sigma = 1$ , and  $\sigma_\epsilon \in (0.01, 0.05)$ . This is the same setup that was used for simulations in Section 2. For each configuration, we generated 200 two-dimensional datasets on a time grid from 0 to 1000, with sampling interval 5. The resulting data has length  $n = 200$ .

Figure 2 presents the violin plots of the composite likelihood estimates of the 200 replicates in comparison to the true values of the four parameters. Violin plots are similar to box plots with a rotated kernel density plot on each side. The horizontal bars in the panels are the true parameter values. For each parameter, the true value lies in the bulk part of the violin plot. This indicates that the true parameters are recovered well by both MCLE methods. The left and right panels have different size of added measurement errors. The variation of the estimates in the case of  $\sigma_\epsilon = 0.01$  is noticeably smaller than that in the case of  $\sigma_\epsilon = 0.05$ , which is expected.

The second simulation study addresses the problem of estimating of standard errors for both MCLE procedures via parametric bootstrap. The sampling horizon (the length of observation window) is set to two levels, 200 and 500 time units. The sampling interval (the inverse sampling frequency) also have two levels, 1 and 5 time units. The parameters of MRME process are:  $\lambda_1 = 1$ ,  $\lambda_0 = 0.5$ ,  $\sigma = 1$ , and  $\sigma_\epsilon = 0.01$ . The result of simulation is recorded in Table 2. Once again we can see that both the marginal method and the two-piece method recover the true parameters well. Their empirical standard errors are similar. This tells us that two methods have comparable efficiency for these setups. Moreover, the

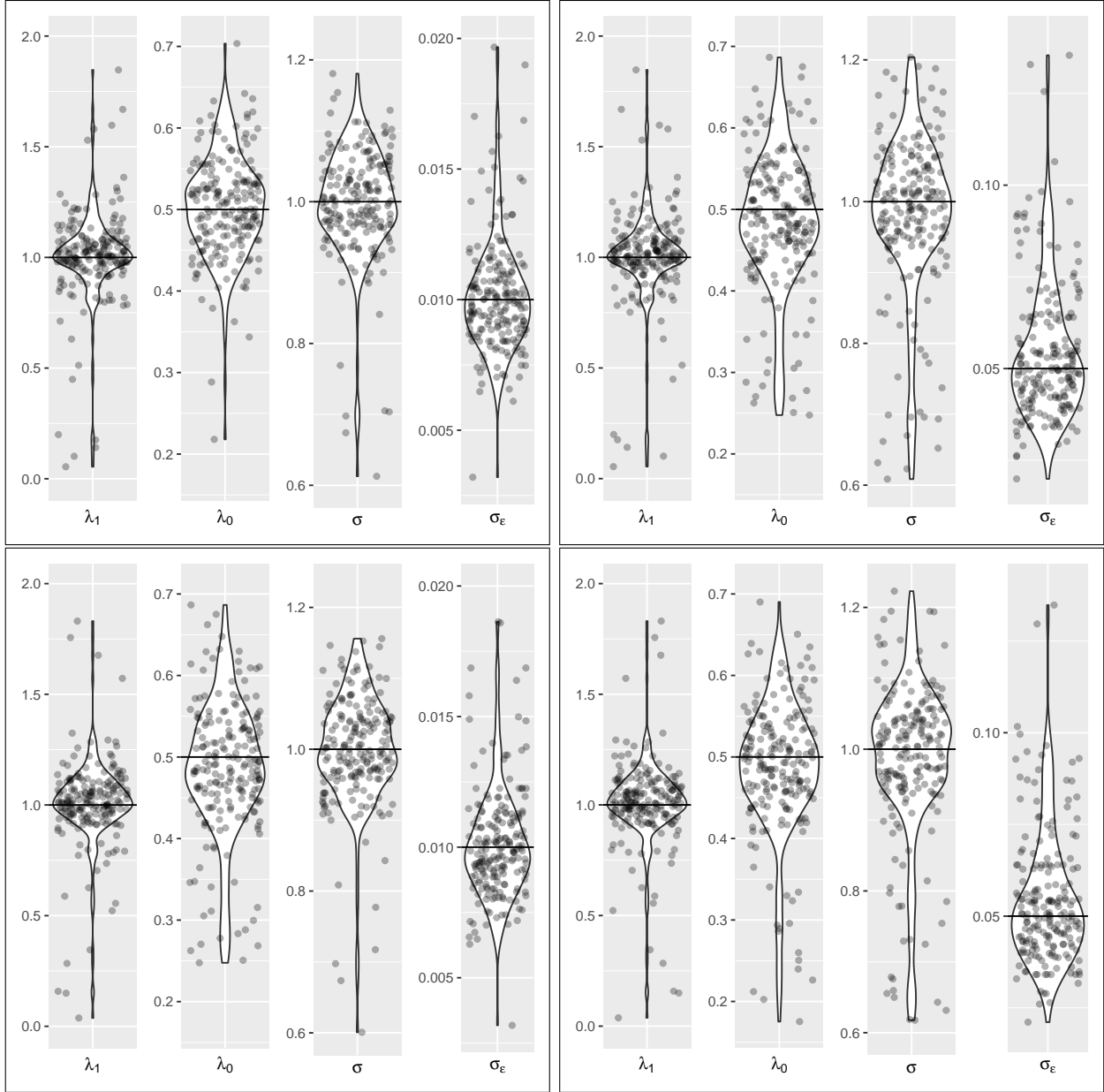


Figure 2: Violin plots of the MCLE with two-piece method (*top*) and marginal method (*bottom*) from 200 replicates. The horizontal bar in each panel is the true parameter value  $\lambda_1 = 1$ ,  $\lambda_0 = 0.5$ ,  $\sigma = 1$ , and  $\sigma_\epsilon = 0.01$  (*left*) and  $0.05$  (*right*). The number of replications is 200.

standard errors were estimated by parametric bootstrap procedure. As we can see, the estimated standard errors are reasonably close to empirical ones.

Finally, let us note that the performance of two methods is similar in two simulation studies described above. It is a bit surprising because the marginal method basically ignores

Table 2: Summaries of average estimator (EST), empirical standard error (ESE), and average parametric bootstrap standard error (ASE) of maximum composite likelihood estimator with two-piece method (Formula (3)) and marginal method (Formula (4)). The number of replications is 200.

Sampling horizon	Sampling interval	Parameter	True value	Two-piece method			Marginal method		
				EST	ESE	ASE	EST	ESE	ASE
200	1	$\lambda_1$	1.0	1.104	0.394	0.386	1.057	0.410	0.414
		$\lambda_0$	0.5	0.502	0.093	0.092	0.488	0.109	0.109
		$\sigma$	1.0	1.011	0.084	0.088	1.001	0.089	0.097
		$\sigma_\epsilon(\times 10^{-2})$	1.0	1.002	0.070	0.068	1.002	0.069	0.068
	5	$\lambda_1$	1.0	0.961	0.546	0.508	0.982	0.570	0.516
		$\lambda_0$	0.5	0.493	0.169	0.240	0.485	0.211	0.251
		$\sigma$	1.0	0.966	0.189	0.163	0.970	0.194	0.166
		$\sigma_\epsilon(\times 10^{-2})$	1.0	1.145	0.710	0.651	1.136	0.665	0.648
500	1	$\lambda_1$	1.0	1.038	0.240	0.224	0.983	0.225	0.223
		$\lambda_0$	0.5	0.508	0.060	0.058	0.495	0.065	0.062
		$\sigma$	1.0	1.008	0.060	0.055	0.997	0.067	0.058
		$\sigma_\epsilon(\times 10^{-2})$	1.0	0.998	0.044	0.042	0.998	0.044	0.042
	5	$\lambda_1$	1.0	1.020	0.362	0.342	1.009	0.354	0.335
		$\lambda_0$	0.5	0.512	0.101	0.111	0.509	0.106	0.115
		$\sigma$	1.0	0.982	0.122	0.114	0.978	0.119	0.112
		$\sigma_\epsilon(\times 10^{-2})$	1.0	1.046	0.356	0.376	1.045	0.362	0.357

the dependence of the MRME process and treats its increment as they are independent. One possible explanation is that if the distance between two consecutive observation is relatively long then the dependence between two consecutive increments of the MRME process is weaker. To see that one can easily calculate the correlation of absolute values of consecutive increments via simulation by employing the auto-correlation function with lag 1 (ACF(1)). For example, for the same parameter set as in the above simulations and a long time horizon 100000, the ACF(1) for the sampling interval 5 is 0.02, but the ACF(1) for the sampling interval 0.1 is 0.46. The results of simulation with small sampling interval 0.1 are presented in Table 3. This simulation suggests that the two-piece procedure is preferable for datasets with shorter sampling intervals (more frequent observations).

Table 3: Summaries of average estimator (EST) and empirical standard error (ESE) of maximum composite likelihood estimator for two-piece method (Formula (3)) and marginal method (Formula (4)). The number of replications is 200.

Sampling horizon	Sampling interval	Parameter	True value	Two-piece method		Marginal method	
				EST	ESE	EST	ESE
200	0.1	$\lambda_1$	1.0	1.031	0.238	1.132	0.329
		$\lambda_0$	0.1	0.102	0.024	0.109	0.026
		$\sigma$	1.0	1.002	0.040	1.007	0.043
		$\sigma_\epsilon (\times 10^{-2})$	1.0	0.999	0.015	0.999	0.015

## 6 Movement of Mountain Lion

The MRME model was applied to the global positioning system (GPS) data of a mature female mountain lion living in the Gros Ventre Mountain Range near Jackson Wyoming. The data were collected by a code-only GPS wildlife tracking collar from 2009 to 2012. The collar was designed to record the location every 8 hours, but the actual sampling intervals were irregular. The movement behaviors of mountain lions are known to be different across seasons. So, we fitted a MRME model to the summer data (from June 1, 2012 to August 31, 2012) and winter data (from December 1, 2011 to February 29, 2012) separately. These two periods of data were plotted as Figure 3. The summer data had an average sampling interval of 5.46 hours with standard deviation 5.14 hours, ranging from 0.5 hours to 32 hours. The average sampling interval is 5.58 hours in the winter data, with standard deviation 4.09 hours and range from 0.5 hours to 25 hours. The summer data has 401 observations and winter data has 392 observations.

The maximum two-piece composite likelihood (Formula (3)) estimates for summer data are  $\hat{\lambda}_1 = 2.841/hour$ ,  $\hat{\lambda}_0 = 0.179/hour$ ,  $\hat{\sigma} = 1.335km/hour^{1/2}$  and  $\hat{\sigma}_\epsilon = 0.019km$ . On average, this female mountain lion stays in moving and resting for 0.352 hours and 5.587 hours during summer and if it keeps moving for one hour, the average deviation from the initial position is 1.335km in both directions (northing and easting). Compared to summer data, the estimates for winter data are  $\hat{\lambda}_1 = 6.225/hour$ ,  $\hat{\lambda}_0 = 0.118/hour$ ,  $\hat{\sigma} = 1.506km/hour^{1/2}$

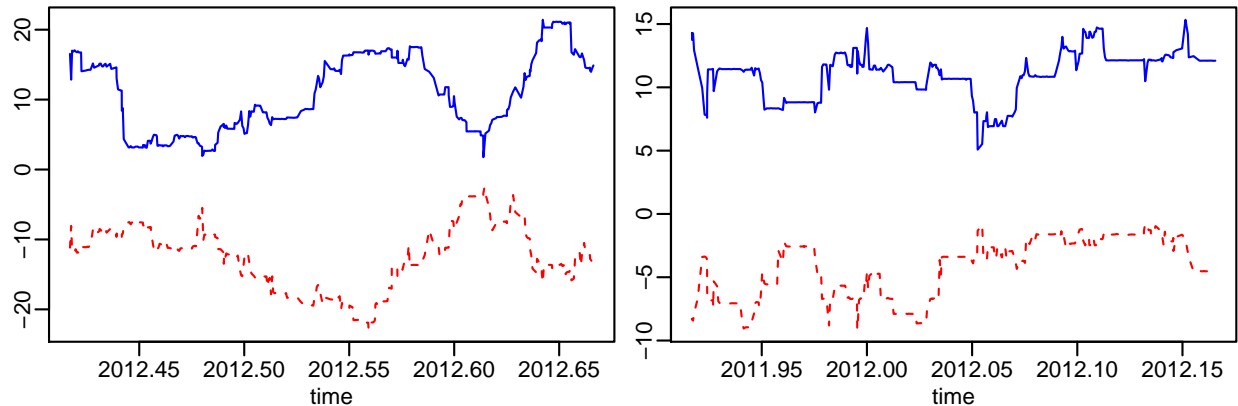


Figure 3: Actual coordinates of a female mountain lion in the Gros Ventre mountain range, Wyoming. The x-axis is time in years. The y-axis is departure from the starting point. The solid blue line is UTM easting ( $km$ ) and the dashed red line is UTM northing ( $km$ ). *Left*: Summer period data, from June 1, 2012 to August 31, 2012. *Right*: Winter period data, from December 1, 2011 to February 29, 2012.

Table 4: Analysis results for mountain lion movement data. Point estimates (EST) from both two-piece method and marginal method are reported. Standard error of point estimates are evaluated by parametric bootstrap (SE).

Season	Parameter	Two-piece method		Marginal method	
		EST	SE	EST	SE
Summer	$\lambda_1$	2.841	0.459	1.090	0.280
	$\lambda_0$	0.179	0.014	0.158	0.015
	$\sigma$	1.335	0.106	0.999	0.104
	$\sigma_\epsilon (\times 10^{-2})$	1.854	0.087	1.879	0.078
Winter	$\lambda_1$	6.225	0.825	4.720	0.711
	$\lambda_0$	0.118	0.010	0.114	0.009
	$\sigma$	1.506	0.095	1.454	0.089
	$\sigma_\epsilon (\times 10^{-2})$	0.908	0.036	0.934	0.043

and  $\hat{\sigma}_\epsilon = 0.009km$ . It is clearly to see that during winter period this female mountain lion spends 51.7% more time in each staying and 54.4% less time in each moving. The mobility keeps comparable. The estimate of  $\sigma_\epsilon$  (standard deviation of Gaussian noise) indicates that the GPS tracking collar has about 10 to 20 meters measurement error and the error is twice higher in summer than it in winter, that is consistent to the knowledge from ecologist (Owari et al., 2009). The result from marginal method is similar (Table 4).

## 7 Discussion

Inactive periods and measurement errors are both desired features of animal movement models. Handling measurement errors added to the MR process is especially critical because, if discarded, a microscopic amount of measurement error would cause substantial bias in estimation. Rounding the observed data is too ad hoc. The issue is rooted in that the flat pieces in the trajectory of an MR process would disappear when noises are present. Our approach based composite likelihood is the first to make the MRME model practically feasible. For movement data from predators that are known to have long inactive periods, the MRME model has great potential in revealing insights for animal ecologists.

The MRME model can be extended to meet further practical needs. For some predators, an inactive period may have different purposes such as resting and food handling for predators. [Pozdnyakov et al. \(2020\)](#) introduced the moving-resting-handling (MRH) process that allows two different types of motionless states. Introducing measurement errors to the MRH model would be useful. Nonetheless, even without measurement errors, evaluating the likelihood of the MRH model is extremely computationally demanding. The moving period may be of different types too to accommodate different moving behaviors ([Benhamou, 2011](#); [Kranstauber et al., 2012](#)). This can be done by allowing the volatility parameter to have multiple levels. More generally, it can depend on terrain, weather conditions, or other covariates. Our MRME model provides a benchmark for these more realistic extensions.

## References

- Andrieu, C., A. Doucet, and R. Holenstein (2010). Particle Markov chain Monte Carlo methods. *Journal of the Royal Statistical Society: Series B (Statistical Methodology)* 72(3), 269–342.
- Benhamou, S. (2011, 01). Dynamic approach to space and habitat use based on biased random bridges. *PLoS ONE* 6(1), e14592.

- Brillinger, D. R. (2010). Modeling spatial trajectories. In A. E. Gelfand, P. J. Diggle, M. Fuentes, and P. Guttorp (Eds.), *Handbook of Spatial Statistics*, pp. 463–476. Chapman & Hall/CRC Boca Raton, Florida, USA.
- Cagnacci, F., L. Boitani, R. A. Powell, and M. S. Boyce (2010). Animal ecology meets GPS-based radiotelemetry: A perfect storm of opportunities and challenges. *Philosophical Transactions of the Royal Society B: Biological Sciences* 365(1550), 2157–2162.
- Cappé, O., E. Moulines, and T. Rydén (2005). *Inference in Hidden Markov Models*. Springer.
- Godambe, V. P. (1960, 12). An optimum property of regular maximum likelihood estimation. *Ann. Math. Statist.* 31(4), 1208–1211.
- Hooten, M. B., D. S. Johnson, B. T. McClintock, and J. M. Morales (2017). *Animal Movement: Statistical Models for Telemetry Data*. CRC Press.
- Horne, J. S., E. O. Garton, S. M. Krone, and S. Lewis, J (2007). Analyzing animal movements using Brownian bridges. *Ecology* 88(9), 2354–2363.
- Hu, C., V. Pozdnyakov, and J. Yan (2019, Sep). Density and distribution evaluation for convolution of independent gamma variables. *Computational Statistics*. to appear.
- Ionides, E. L., A. Bhadra, Y. Atchadé, and A. King (2011). Iterated filtering. *The Annals of Statistics* 39(3), 1776–1802.
- Ionides, E. L., D. Nguyen, Y. Atchadé, S. Stoev, and A. A. King (2015). Inference for dynamic and latent variable models via iterated, perturbed Bayes maps. *Proceedings of the National Academy of Sciences* 112(3), 719–724.
- Jonsen, I. D., J. M. Flemming, and R. A. Myers (2005). Robust state-space modeling of animal movement data. *Ecology* 86(11), 2874–2880.
- King, A. A., D. Nguyen, and E. L. Ionides (2016). Statistical inference for partially observed Markov processes via the R package pomp. *Journal of Statistical Software* 69(12), 1–43.



- Kranstauber, B., R. Kays, S. D. LaPoint, M. Wikelski, and K. Safi (2012). A dynamic brownian bridge movement model to estimate utilization distributions for heterogeneous animal movement. *Journal of Animal Ecology* 81(4), 738–746.
- Lindsay, B. G. (1988). Composite likelihood methods. *Contemporary Mathematics* 80, 221–239.
- Mashanova, A., T. H. Oliver, and V. A. Jansen (2010). Evidence for intermittency and a truncated power law from highly resolved aphid movement data. *Journal of The Royal Society Interface* 7(42), 199–208.
- McClintock, B. T., R. King, L. Thomas, J. Matthiopoulos, B. J. McConnell, and J. M. Morales (2012). A general discrete-time modeling framework for animal movement using multistate random walks. *Ecological Monograph* 82, 335–349.
- Owari, T., H. Kasahara, N. Oikawa, and S. Fukuoka (2009, 01). Seasonal variation of global positioning system (gps) accuracy within the tokyo university forest in hokkaido. *Bulletin of Tokyo University Forests* 120, 19–28.
- Patterson, T., L. Thomas, C. Wilcox, O. Ovaskainen, and J. Matthiopoulos (2008). State-space models of individual animal movement. *Trends in Ecology and Evolution* 23(2), 87–94.
- Patterson, T. A., A. Parton, R. Langrock, P. G. Blackwell, L. Thomas, and R. King (2017). Statistical modelling of individual animal movement: An overview of key methods and a discussion of practical challenges. *Advances in Statistical Analysis* 101(4), 399–438.
- Pozdnyakov, V., L. Elbroch, C. Hu, T. Meyer, and J. Yan (2020). On estimation for brownian motion governed by telegraph process with multiple off states. *Methodology and Computing in Applied Probability*.

- Pozdnyakov, V., L. Elbroch, A. Labarga, T. Meyer, and J. Yan (2019, Sep). Discretely observed brownian motion governed by telegraph process: Estimation. *Methodology and Computing in Applied Probability* 21(3), 907–920.
- Pozdnyakov, V., T. H. Meyer, Y.-B. Wang, and J. Yan (2014). On modeling animal movements using brownian motion with measurement error. *Ecology* 95, 247–253.
- Preisler, H. K., A. A. Ager, B. K. Johnson, and J. G. Kie (2004). Modeling animal movements using stochastic differential equations. *Environmetrics* 15(7), 643–657.
- Ueno, T., N. Masuda, S. Kume, and K. Kume (2012). Dopamine modulates the rest period length without perturbation of its power law distribution in *Drosophila melanogaster*. *PLoS One* 7(2), e32007.
- Varin, C., N. Reid, and D. Firth (2011). An overview of composite likelihood methods. *Statistica Sinica* 21(1), 5–42.
- Yan, J., Y.-W. Chen, K. Lawrence-Apfel, I. Ortega, V. Pozdnyakov, S. Williams, and T. Meyer (2014). A moving-resting process with an embedded Brownian motion for animal movements. *Population Ecology* 56(2), 401–415.
- Yan, J., V. Pozdnyakov, and C. Hu (2019). *smam: Statistical Modeling of Animal Movements*. R package version 0.4.0.9000 (GitHub: <https://github.com/ChaoranHu/smam>).
- Zacks, S. (2004). Generalized integrated telegraph processes and the distribution of related stopping times. *Journal of Applied Probability* 41(2), 497–507.

## A Formulas for High Dimension

Let  $\mathbf{X}(t_k)$  and  $\mathbf{Z}(t_k)$  be  $d$ -dimensional random vectors. Set  $\mathbf{X}(t_k) = (X_1(t_k), \dots, X_d(t_k))$ ,  $\epsilon_{\mathbf{k}} = (\epsilon_{1k}, \dots, \epsilon_{dk}) \sim MN(\mathbf{0}, \sigma_\epsilon^2 \mathbf{I})$ , and  $\epsilon_i$  and  $\epsilon_j$  are independent for  $i \neq j$ . Then,  $\mathbf{Z}(t_k) =$

$(Z_1(t_k), \dots, Z_d(t_k)) = (X_1(t_k) + \epsilon_{1k}, \dots, X_d(t_k) + \epsilon_{dk})$ . The density  $h_{ij}$  is the  $d$ -dimension case is given by

$$h_{10}(\mathbf{x}, t) = \int_0^t \prod_{i=1}^d \phi(x_i; \sigma^2 w) p_{10}(w, t) dw.$$

Then we get that

$$\begin{aligned} g_{10}(\mathbf{z}, t) &= \int_{\mathbb{R}} \dots \int_{\mathbb{R}} h_{10}(\mathbf{z} - \mathbf{x}; \sigma^2 w) \prod_{i=1}^d \phi(x_i; 2\sigma_\epsilon^2) dx_1 \dots dx_d \\ &= \int_{\mathbb{R}} \dots \int_{\mathbb{R}} \left[ \int_0^t \prod_{i=1}^d \phi(z_i - x_i; \sigma^2 w) p_{10}(w, t) dw \right] \prod_{i=1}^d \phi(x_i; 2\sigma_\epsilon^2) dx_1 \dots dx_d \\ &= \int_0^t \prod_{i=1}^d \left[ \int_{\mathbb{R}} \phi(z_i - x_i; \sigma^2 w) \phi(x_i; 2\sigma_\epsilon^2) dx_i \right] p_{10}(w, t) dw. \end{aligned}$$

Similarly, we also have

$$\begin{aligned} g_{00}(\mathbf{z}, t) &= \int_0^t \prod_{i=1}^d \left[ \int_{\mathbb{R}} \phi(z_i - x_i; \sigma^2(t-w)) \phi(x_i; 2\sigma_\epsilon^2) dx_i \right] p_{00}(w, t) dw + e^{-\lambda_0 t} \prod_{i=1}^d \phi(z_i, 2\sigma_\epsilon^2), \\ g_{01}(\mathbf{z}, t) &= \int_0^t \prod_{i=1}^d \left[ \int_{\mathbb{R}} \phi(z_i - x_i; \sigma^2(t-w)) \phi(x_i; 2\sigma_\epsilon^2) dx_i \right] p_{01}(w, t) dw, \\ g_{11}(\mathbf{z}, t) &= \int_0^t \prod_{i=1}^d \left[ \int_{\mathbb{R}} \phi(z_i - x_i; \sigma^2 w) \phi(x_i; 2\sigma_\epsilon^2) dx_i \right] p_{11}(w, t) dw \\ &\quad + e^{-\lambda_1 t} \prod_{i=1}^d \left[ \int_{\mathbb{R}} \phi(z_i - x_i; \sigma^2 t) \phi(x_i; 2\sigma_\epsilon^2) dx_i \right]. \end{aligned}$$

Let us mention that these formulas do not require numerical multiple integral evaluation and, as a consequence, are computationally efficient.